A LARGE SIGNAL EQUIVALENT CIRCUIT MODEL FOR MULTIELECTRODE LASER AND MICROWAVE SEMICONDUCTOR LASERS FOR CAD APPLICATIONS

H. ELKADI, S.MARICOT, R.HAMELIN, J.HARARI, J.P.VILCOT, D.DECOSTER

Institut d'Electronique et de Microélectronique du Nord, IEMN, DHS
Université des Sciences et Technologies de Lille, FRANCE

ABSTRACT

We present an equivalent circuit large signal model of semiconductor lasers for microwave applications. The model is implemented on SPICE software and is based on a modified set of the monomode rate equations. The carriers density in the active region is related to the potential at the terminals of the active region by a polynomial approximation of the Fermi Integral. Different recombination mechanisms (Schockley-Hall-Read, spontaneous and Auger) are represented by separate terms and not as a global constant life time. The model also accounts for saturable aborption occuring in the case of multielectrode lasers. Different applications are presented. A study of the behaviour of a multielectrode laser with saturable absorbers, under static, transient and small signal conditions is performed. The study shows the bistability of this type of lasers and predicts an extremely wide band up to the millimetric frequencies range. Another application of the model is the matching of the impedance of the laser to the 50Ω of the microwave source; using passif reactive circuit.

DEFINITION TABLE

n, N_o	:	carriers density, static carriers density
N_{om}	:	carriers density for transparency ($1x10^{18}cm^{-3}s^{-1}$)
n_1, s_1, α_1	:	perturbation excess carriers density, photons density and absorption
S, S_o	:	photons density, static photons density
I	:	injected current
g	:	optical differential gain ($1.0x10^{-6}cm^3s^{-1}$)
ε	:	optical gain saturation coefficient ($2x10^{-23}cm^3$)
Γ	:	optical confinement factor (0.2)
W,d	:	Width (2μm), depth (0.036μm) of the optical cavity
L_o, L_e, L_{abs}	:	Length of the optical cavity (500μm), the bias electrode (440μm), and the absorber section (2x6μm)
β	:	percentage of the spontaneous emission entering in the lasing action (10^{-5})
A_{nr}, B_{sp}, C_a	:	non radiative ($1x10^8s^{-1}$), spontaneous ($1x10^{-10}cm^3s^{-1}$), and Auger ($7x10^{-29}cm^6s^{-1}$) recombination coefficients.
v_g	:	group velocity of the laser mode ($\approx 0.75x10^{10}cm\ s^{-1}$)
α_b	:	total absorption and losses within the laser cavity ($40cm^{-1}$)
α_m	:	distributed mirror losses = $\ln(1/R) / L_o$
R_f, R_r	:	front and rear mirror reflectivity $R_f=R_r=R=0.3$
Φ_e	:	cavity electrical volume = $WxdxL_e$
Φ_o	:	cavity optical volume = $WxdxL_o$
α_{abs}	:	absorption coefficient in the absorber section
$\alpha_{so}, \alpha_{nso}$	:	maximum saturable ($2x10^4cm^{-1}$) and non-saturable ($1.5x10^3cm^{-1}$) absorption coefficients
$\kappa_1, \kappa_2, \kappa_3$	:	Voltage normalization constants (all three taken to be equal to 1.25)
S_{so}	:	Saturation photons density ($\sim 1x10^{20}cm^{-3}$)

1. INTRODUCTION

Microwave optical fiber links present a very interesting solution for microwave communications in vertue of their low loss and their large bandwidth compared to conventional transmission lines; as well as their small size, immunity to EMI and tapping. Nevertheless, optical links are limited by the laser bandwidth, its chirping, non-linearities, as well as its low impedance level. In order to solve these problems, an adequate model of the laser is required. An equivalent circuit large signal model of the laser would allow the study of the behaviour of the laser within the optical link, taking into account its structure, as well as its parasitics. Such models were previously presented [1,2], however most of them represent the laser electrically as an ideal diode and/or represent the different recombination mechanisms in the active region by a constant life time. The first assumption (ideal diode) can hardly be justified since the high carriers density in a laser requires the use of Fermi-Dirac statistics due to the carriers degeneracy; while the second (constant life time) can not be applied to the case of the multielectrode lasers, where large variations of carriers concentration accompany the change of the material absorption.

OF1

CH3277-1/93/0000-0217$01.00 © 1993 IEEE

2. THE MODEL

The behaviour of the semiconductor laser diodes is described, in a classical approach, by the well known monomode rate equations;

$$\frac{dn}{dt} = \frac{I}{q\Phi_e} - g\,(n - N_{om})(1-\varepsilon S)S - (A_{nr}n + B_{sp}n^2 + C_a n^3) \quad (1)$$

$$\frac{dS}{dt} = \Gamma g\,(n - N_{om})(1-\varepsilon S)S + \beta B_{sp}n^2 - v_g(\alpha_b + \alpha_m)S \quad (2)$$

However, these equations were developed for the case where the current flows uniformly in all the optical cavity. In the case of multielectrode lasers, the current flows only in the regions under the contacts; that is, if we neglect the lateral diffusion of the carriers, except for being responsible for the transparency of the cavity in the spacing between contacts. This results in two different cavity volumes: electrical and optical. Moreover, an extra source of absorption is to be accounted for; namely the band to band absorption in the absorber region of the cavity. The rate equations can thus be rewritten for the conservation of the total number of carriers and photons, yielding:

$$q\Phi_e\frac{dn}{dt} = I - q\Phi_e\, g\,(n - N_{om})(1-\varepsilon S)S - q\Phi_e(A_{nr}n + B_{sp}n^2 + C_a n^3) \quad (3)$$

$$\frac{q\Phi_o}{\Gamma}\frac{dS}{dt} = q\Phi_e\, g\,(n - N_{om})(1-\varepsilon S)S + \frac{q\Phi_e}{\Gamma}\beta B_{sp}n^2 - \frac{q\Phi_o}{\Gamma}v_g(\alpha_b + \alpha_m)S - q\Phi_{abs}\, v_g\, \alpha_{abs}\, S \quad (4)$$

where α_{abs} can be expressed as

$$\alpha_{abs} = \frac{\alpha_{so}\,(1 - \kappa_1 V_{abs})}{1 + \frac{S}{S_{so}(1-\kappa_2 V_{abs})}} + \alpha_{nso}\,(1 - \kappa_3 V_{abs}) \quad (5)$$

It is worthwhile noting that for a classical structure (with a single electrode), $\Phi_o = \Phi_e$ and $\Phi_{abs} = 0$, and we obtain equations (1) and (2). This form of absorption [equation (5)], accounts for the decrease of absorption with the applied potential. Application of a forward bias results in the injection of carriers in the active region; thus partially filling the available states in the conduction band of the active region quantum wells (electrical pumping) and decreasing the absorption coefficient. Expression (5) also reflects the saturation of absorption with increasing photons density. Increasing photons density results in larger electrons transfer to the conduction band due to the electron-hole pairs created by photons absorption (similar to optical pumping) and consequently has a similar effect on the absorption as the carrier injection. The saturation photons density decreases with applied potential since, simply, the available states in the conduction band are already partially filled due the electrically injected carriers. A more rigorous approach would state that a part of the absorbed photons are compensated by re-emission, thus reducing the material effective absorption. The α_{nso} term accounts for the non-saturable absorption and losses dependence on the applied potential. The losses can be in part attributed to the light diffraction and attenuation due to the carriers induced difference of the refractive index in the absorber section.

As for the carriers density representation in the model, a polynomial development of the Fermi Integral allows us to substitute n by V, the terminal applied potential, and thus obtaining a set of equations analogous to circuit equations. Once the photons density S is expressed in terms of the output power per facet, using the relation:

$$P = 0.5\,\Phi\eta/\Gamma\tau_p q E_g S \quad (6)$$

the above system of equations can be solved by any non linear circuit simulator. Fig 1 shows the equivalent circuit obtained. In our case, the PSPICE commercial software was utilized to obtain the results presented in the next section.

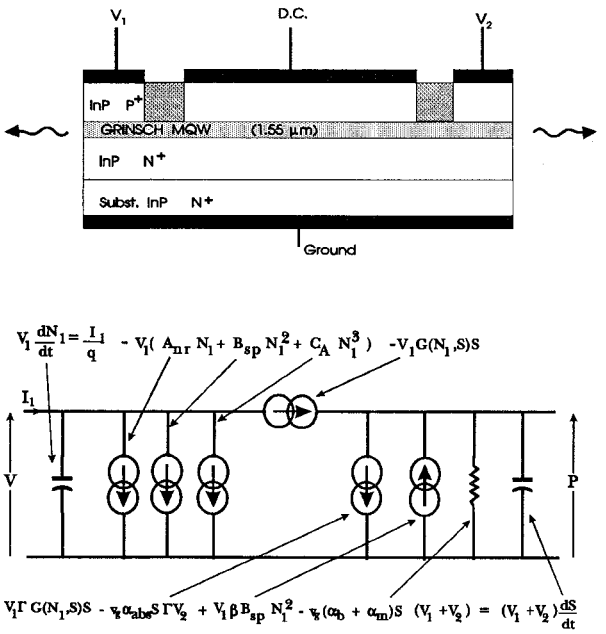

Fig.1. Schematic structure of the multielectrode laser and the corresponding equivalent

3. APPLICATIONS

3.1 Multielectrode lasers

Using the values given in the definition table for the 3-quantum well 500 µm long 1.5µm wavelength laser reported in [3,4], we obtain, under dc conditions, the P-I characteristic shown in fig.2. The results shown here are in a good agreement with those reported in [1].

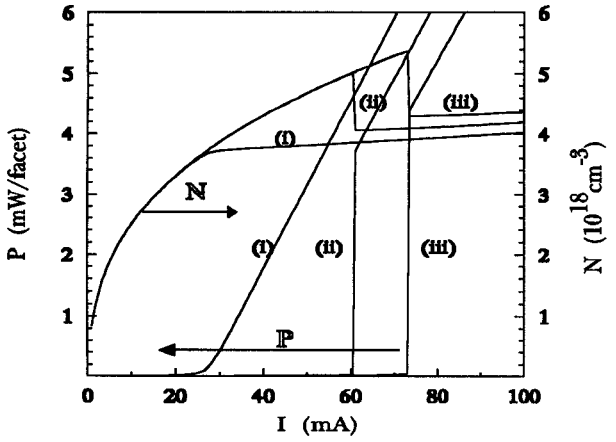

Fig.2. Stimulated light power vs current characteristic and the corresponding carriers concentration evolution in the gain section for (i) $V_{abs1}=V_{abs2}=0.8V$, (ii) $V_{abs1}=V_{abs2}=0.4V$, (iii) $V_{abs1}=0$, $V_{abs2}=0.8V$

Fig.2 also shows the evolution of the carriers density within the gain section with current for different absorber voltages. It can be noted that the carriers density increases with decreasing absorber potential and that this density is significantly higher than in cases of classical lasers, in order to compensate the losses in the absorber section. This justifies the assumption that carriers lateral diffusion is sufficient to banish the absorption in the inter-electrode spacing. It is however to be noted that the case of V_{abs} = 1V is not simulated; since in this case the absorber region becomes amplifying due to population inversion; a case which requires a different formulation of the problem. In fact, for a potential of 0.8V, the carriers density in the active region is around $10^{18}cm^{-3}$ which is the density for transparency, justifying the values used for the dependence of the saturable absorber on the applied voltage.

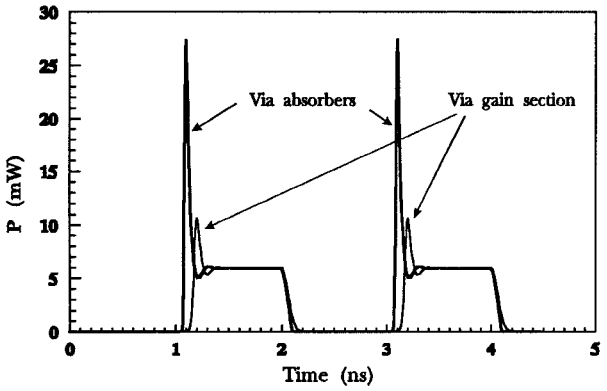

Fig.3. Transient response of the laser modulated via the gain and the absorber sections

Fig.3 shows the transient response of the multielectrode laser subject to a square wave signal applied to the absorber section. It is to be noted that the overshoot of the power intensity is very large relative to that obtained by bias current modulation and that the damping of the relaxation oscillations of the laser is significantly stronger. The higher overshoot is due to the fact that, in this case, the population inversion is allowed to reach much higher values as can be seen from fig.2 , and that the photons density is directly modified by the change of the absorption while in the case of current modulation, the carriers density increase is smoothed by the relaxation mechanisms and consequently the optical gain increase is not as abrupt as that of absorption. The higher damping would be due to the Auger recombination [5] which becomes dominant in the case of high carriers densities as in this case.

The high overshoot amplitude can be related to the small signal frequency response resonance amplitude. Fig.4 shows the frequency responses for the same laser modulated by two different techniques; gain section current modulation (solid line) and absorer section modulation (dotted line). It is clear that the two curves have the same resonance frequency, however, the former has a higher resonance amplitude and, more interesting, a -20dB/decade slope afterwards instead of the known -40dB/decade for current modulation. This behaviour can be predicted using the small signal expression:

$$H(\omega)=\frac{S_1}{\alpha_1(V)}=-\frac{G\frac{\Phi_{abs}}{\Phi_o}v_g S_o\left(j\omega+gS_o+\frac{1}{\tau_n}\right)}{\frac{gS_o}{\tau_p}-\omega 2+j\omega\left(gS_o+\frac{1}{\tau_n}\right)} \qquad (7)$$

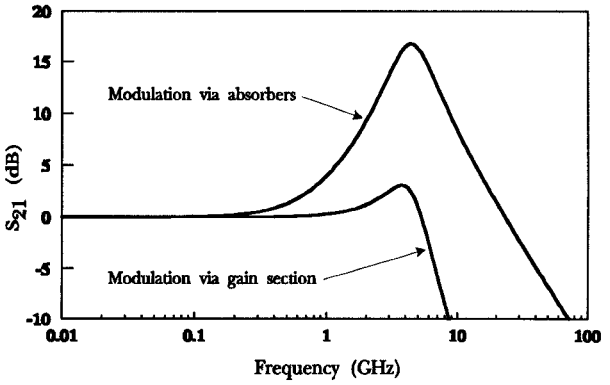

Fig.4 Small signal frequency response of the laser modulated via the gain and the absorber sections.

The derivation of which is given in [6]. This, as can be obviously seen, leads to a higher cut-off frequency. From this point of view, the modulation via absorption may be very promising for microwave modulation up to the millimetric range. The predicted cut-off frequency for I= 50mA is around 32GHz in contrast with 7GHz for gain section current modulation and the resonance frequency for both modulation techniques is about 4.3GHz.

3.2 Impedance matching and optical link modeling

Another application of the model os the design of a microwave optical fiber link. The laser used is modeled using its static and dynamic characteristics as well as its structure, the parasitic elements are determined from the measured S parameters of the laser diode using the EESOF Touchstone circuit simulation software, and a reactive matching network is designed and implemented successfully [7]. The laser model was used to simulate the entire link. Fig. 5. shows a schematic of the optical link, the modeled as well as the measured S21 parameters of the matched as well as non matched link. An improvement of 12dB can be observed and a good match between modeled and experimental results is obtained.

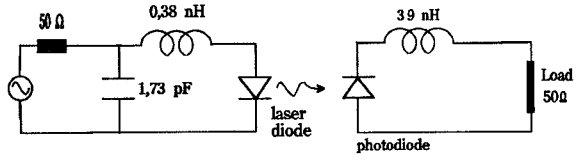

(a) matched optical link

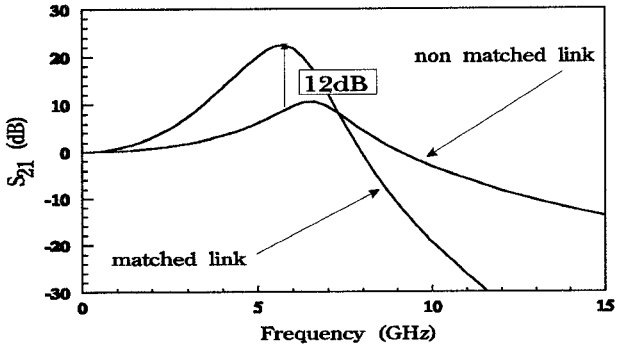

(b) Modeled S21 parameter of the optical link

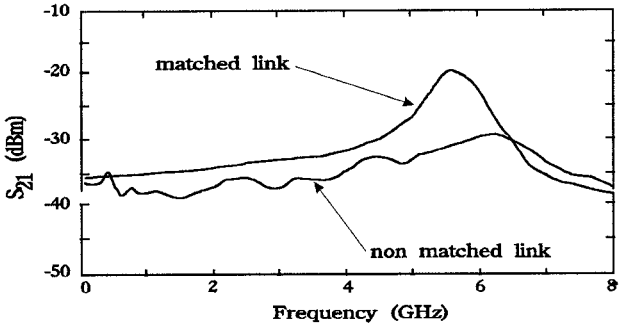

(c) Measured S21 parameter of the optical link

Fig.5 Impedance matching of a microwave optical link

The laser parasitics are found to be very large compared to the laser intrinsic impedance. The fraction of the power actually delivered to the active layer is found to be less 5% of the total power consumed by the laser diode. A laser with high intrinsic input impedance is then necessary to improve the power transfer efficiency. The multielectrode lasers may present such a solution since the absorbers can be biased below threshold and consequently present higher input impedance.

4. CONCLUSION

We have presetned an equivalent circuit model of semiconductor lasers. The model can be applied for the study of the behaviour of new structures such as the multielectrode laser, as well as the simulation of a classical laser (single electrode laser) within an optical link. The resutls obtained are in good agreement with experimental ones and demonstrate the utility of the model. An important result is the possibility of operating multielectrode lasers at extremely high frequencies up to the millimetric frequencies range. It is planned to introduce the noise modeling to the actual model so as to be able to model the laser as well as the optical link noise performance.

REFERENCES

1. R.S.Tucker, " Large Signal Circuit Model for Simulation of .Injection Laser Modulation dynamics," IEEE Proc., Vol. 128, Pt. I, No. 5, October 1981, pp.180

2. W.I. Way, " Large Signal Non-Linear Distortion for Single Mode Laser Diode under Microwave Intensity Modulation," IEEE J. Lightwave Technology., Vol. LT-5, No.3, March 1987, pp.305.

3. A.F.J. Levi et al., "Multielectrode quantum well laser for digital switching", Appl. Phys. Lett. 56(12), 1990, pp.1095.

4. J. O'Gorman et al., "Dynamic and static response of multielectrode lasers", Appl. Phys. Lett. 57 (10), 1990, pp.968

5. Ming Tang and Shyh Wang, "Simulation studies of the behavior of semiconductor lasers with Auger recombination",Appl. Phys. Lett. 50 (26), 1987, pp.1861

6. Elkadi et al, "An Equivalent Circuit Model for Multielectrode Lasers: Potential devices for Millimetric Applications", to be published

7. S.Maricot et al.,"Monolithic integration of optoelectronic devices with reactive matching networks for microwave applications," IEEE Photonic Tech. Lett. 4 (11), Nov. 1992